

Ferromagnetic Interactions in Non-Kekulé Polymers

Masashi Hatanaka* **and Ryuichi Shiba**

Department of Materials and Life Sciences, Graduate School of Advanced Science & Technology, Tokyo Denki University, 2-2 Kanda Nishiki-cho, Chiyoda-ku, Tokyo 101-8457

Received June 28, 2007; E-mail: mhatanaka@xug.biglobe.ne.jp

Ferromagnetic interactions in non-Kekulé polymers were analyzed under the periodic boundary condition. We transformed Bloch functions of non-bonding crystal orbitals (NBCOs) into Wannier functions. The product of the ν-th and $(\nu + 1)$-th Wannier functions was defined as $PNBCO_{\nu,\nu+1}$ (product of NBCOs). In so-called nondisjoint-type polymers, ferromagnetic ground states resulted from instabilities of anti-parallel-spin states in $PNBCO_{\nu,\nu+1}$. The instabilities consisted of "on-site term" and "through-space term." The former corresponded to squared amplitude of the same atomic site on $PNBCO_{\nu,\nu+1}$, and the latter corresponded to antibonding-through-space interactions in $PNBCO_{\nu,\nu+1}$. The instabilities led to ferromagnetic-spin alignment. On the other hand, in so called disjoint polymers, such instabilities did not emerge.

Non-Kekulé polymers are π-conjugated polyradicals, of which molecular structures cannot be drawn only by classical C=C double bonds.[1–3] Their ground states have been predicted to be ferromagnetic from the viewpoint of molecular orbital method[1] and valence bond method.[2] **1** described in Fig. 1 is the simplest non-Kekulé polymer, which is an extended system of allyl radical. *N* represents the number of unit cells. In the case of $N = 1$, **1** becomes trimethylenemethane (**2**), which is a well-known triplet biradical with two non-bonding molecular orbitals (NBMOs) and two unpaired electrons.[4–10] The NBMOs can be made to be span the common atoms, and thus, it is called a nondisjoint-type.[4] In general, if two NBMOs of a certain non-Kekulé system can be made to span commom atoms, they are "nondisjoint."[4–6] Oppositely, if the NBMOs cannot be made to span common atoms, they are "disjoint."[4–6] Although the NBMOs are degenerate within the Hückel molecular orbital method, they can be made to minimize the exchange integral by using unitary transformation.[6] Such a pair of NBMOs is a "localized NBMOs," which are localized as much as possible.[6] For example, the localized NBMOs of **2** are shown in Fig. 2. The procedure to obtain localized NBMOs has been established by Aoki and Imamura.[6] They have shown that sum of the squared amplitudes of the localized NBMOs, which has been called L_{ij} index, is approximately proportional to the exchange integral.[6]

Recently, we have introduced the concept of PNBMO, which is a two-electron wave function consisting of the product of localized NBMOs.[11] It has been shown that antibonding-through-space interactions in PNBMO amplitudes contribute to the triplet preference of nondisjoint-type biradicals.[11] The PNBMO of **2** is shown in Fig. 2. In the PNBMO, the antibonding-through-space interactions caused by the out-of-phase moiety "P_{anti}-fragment" destabilize the singlet state, because the Coulomb repulsions of the triplet state are reduced.[11] PNBMO analysis is helpful to understand the origin of ferromagnetic interactions in general nondisjoint biradicals.[11]

Nondisjoint NBMOs result from linkage of "starred atoms" to "unstarred atoms"[4] and resultant orbital mixing.[6] **1** is constructed by this type of linkage, even in the limit of $N \rightarrow \infty$, as shown in Fig. 1. Therefore, chain polymer **1** has infinite nondisjoint NBMOs. Nondisjoint NBMOs lead to high-spin

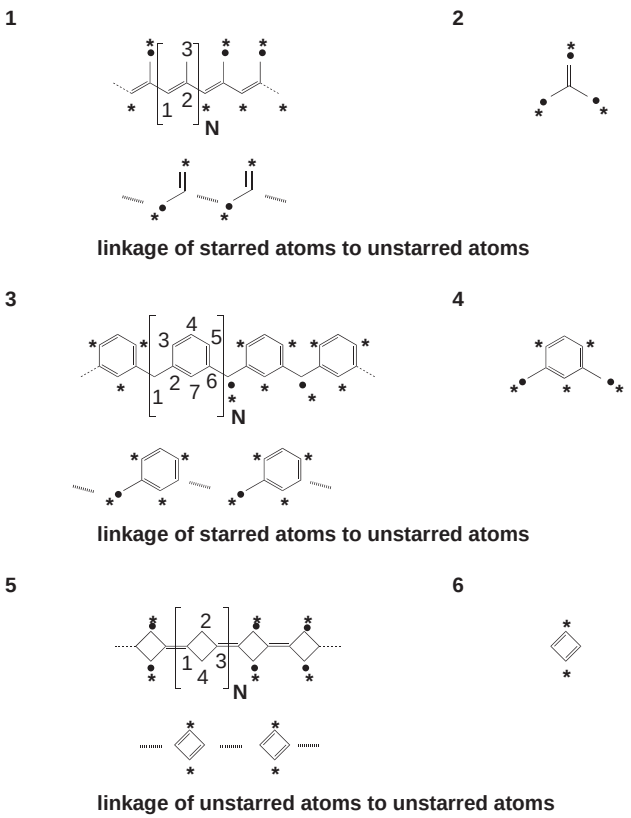

Fig. 1. Molecular structures of the simplest non-Kekulé polymer **1**, trimethylenemethane **2**, poly-*m*-phenylene **3**, *m*-phenylene **4**, polycyclobutadiene **5**, cyclobutadiene **6**. The polymers were treated under the periodic boundary condition.

Published on the web December 13, 2007; doi:10.1246/bcsj.80.2342

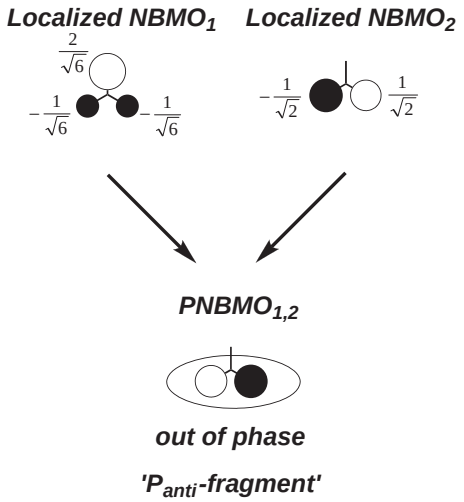

Fig. 2. Localized NBMOs and their product PNBMO of **2**. The out-of-phase moiety "P_{anti}-fragment" contributes to triplet preference.

organic polyradicals. Indeed, **1** has been theoretically predicted to be a ferromagnetic compound with strong spin polarization.[3] Moreover, high-spin states have been observed in heteroatom-containing derivatives of **1**,[12] and there has been increasing interest in high-spin polymer and/or oligomers, of which skeletons are based on **1**.[13,14]

3 in Fig. 1 is also a nondisjoint system known as poly-*m*-phenylene, which is an extended system of benzyl radicals. The skeleton is also constructed by linking the "starred atoms" to the "unstarred atoms." *m*-Phenylene (**4**) in Fig. 1, which corresponds to $N = 1$, is also a triplet biradical.[5] In the case of oligomers with $N > 1$, high-spin states has been theoretically established.[10,15] That is, *m*-phenylene skeleton is a robust ferromagnetic coupler. Tyutyulkov and Karabunarliev have also been predicted the ferromagnetic ground state of **3** by using the Ising Hamiltonian.[16]

5 is another type of non-Kekulé polymer, which has disjoint-type linkage, that is, "unstarred atoms" to "unstarred atoms" as shown in Fig. 1. **5** is regarded as an extended system of singlet biradical cyclobutadienes (**6**),[4,17] and a tetramethyleneethane-type resonance structure can be drawn within each adjacent cell, which is disjoint type.[17] From a theoretical study on oligo-cyclobutadienes,[17] the ground state of **5** has been predicted to be not ferromagnetic.

Thus, nondisjoint NBMOs play an essential role in ferromagnetic spin alignment in non-Kekulé polymers. By using nondisjoint systems, many high-spin polyradicals with large spin-quantum number have been suggested and realized.[9,10,18–21] As for infinite-extended systems, Tyutyulkov and co-workers have clarified the ferromagnetic interactions of many non-Kekulé polymers by using Wannier functions.[16,22] In their treatment, however, amplitude pattern of the Wannier functions is not taken into account, and the Wannier functions are treated so as to be localized only at one unit cell.[16,22] This is inadequate to distinguish magnetic properties of disjoint and nondisjoint systems, because Wannier functions localized only at one unit cell scarcely overlap each other both in disjoint and nondisjoint systems. Thus, we took amplitude-pattern dependence of Wannier functions into account and analyzed ferromagnetic interactions of non-Kekulé polymers. In this process, PNBMO analysis was adapted for chain polymers.

In this paper, the PNBMO concept was theoretically expanded for non-Kekulé polymers under the periodic boundary condition. We transformed the Bloch functions in the nonbonding crystal orbitals (NBCOs) into Wannier functions. The product of the ν-th and $(\nu + 1)$-th Wannier functions was defined as $PNBCO_{\nu,\nu+1}$ (product of NBCOs). It was shown that squared amplitudes of $PNBCO_{\nu,\nu+1}$ represented the instabilities of anti-parallel-spin states of non-Kekulé polymers. In nondisjoint polymers, the instabilities of anti-parallel-spin states consisted of an "on-site term," which corresponded to the squared amplitude on the same atomic site in $PNBCO_{\nu,\nu+1}$, and a "through-space term," which corresponded to the antibonding-through-space interactions in $PNBCO_{\nu,\nu+1}$. On the other hand, in disjoint polymers, both on-site and through-space terms were negligible. A qualitative description of the ferromagnetic interactions in non-Kekulé polymers was emphasized by analyzing nondisjoint polymer **1**, **3**, and disjoint polymer **5**.

Theoretical

In order to explain our method, we first analyzed the simplest non-Kekulé polymer **1**. **1** has NBCOs within the Hückel molecular orbital method. We constructed Bloch functions of the NBCOs and transformed them into Wannier Functions. Wannier functions are suitable for our purpose, because they are localized expression of Bloch functions, analogous to localized NBMOs.[22]

The unit cell of **1** was defined as described in Fig. 1. The numbers 1–3 in the unit cell are index of the carbon atomic sites. The Bloch functions φ_k are expressed by using the NBCOs coefficients $C_r(k)$, which depend on wavenumber k running $-\pi$ to π:

$$\varphi_k = \frac{1}{\sqrt{N}} \sum_{\mu}^{N} \sum_{r}^{n} \exp(ik\mu) C_r(k) \chi_{\mu,r}, \tag{1}$$

where μ and r are indices of unit cell and atomic orbitals therein, respectively. N and n are number of unit cells and atomic orbitals therein, respectively. χ represents the $2p_z$ atomic orbitals. In the case of **1**, r is from 1 to 3. The NBCOs coefficients $C_r(k)$ are obtained by solving secular equation as follows:

$$\begin{vmatrix} x & 1+e^{ik} & 0 \\ 1+e^{-ik} & x & 1 \\ 0 & 1 & x \end{vmatrix} = 0, \tag{2}$$

where x is:

$$x = \frac{\alpha - \varepsilon}{\beta}. \tag{3}$$

α and β are Coulomb and resonance integral, respectively. ε is orbital energy.

From Eqs. 2 and 3, we obtained three energy dispersions as follows:

$$x = 0, \quad x = \pm\sqrt{3 + 2\cos k}. \tag{4}$$

The NBCOs correspond to the dispersion with $x = 0$. The NBCOs coefficients $C_r(k)$ become:

$$C_1(k) = \frac{1}{\sqrt{3 + 2\cos k}}, \tag{5}$$

$$C_2(k) = 0, \tag{6}$$

$$C_3(k) = -\frac{1 + e^{-ik}}{\sqrt{3 + 2\cos k}}. \tag{7}$$

Since $C_r(k)$ generally becomes complex number, we adopt the real part as follows:

$$C'_r(k) = \frac{1}{2}\{C_r(k) + C_r(k)^*\} = \frac{1}{2}\{C_r(k) + C_r(-k)\}, \tag{8}$$

where $C_r(k)^*$ is the complex conjugate of $C_r(k)$, and $C_r(k)^*$ is identical to $C_r(-k)$. This procedure guarantees even-function character of Wannier functions, which is used later.

The Wannier functions are obtained by the following transformation:[16]

$$\psi_\nu = \sum_\mu^N \sum_r^n a_r(\mu - \nu)\chi_{\mu,r}, \tag{9}$$

where $a_r(\mu - \nu)$ is:

$$a_r(\mu - \nu) = \frac{1}{2\pi}\int_{-\pi}^{\pi} \exp\{i(\mu - \nu)k\}C'_r(k)\mathrm{d}k, \tag{10}$$

in the limit of $N \to \infty$.

The coefficient $a_r(\mu - \nu)$ depends on only the difference $(\mu - \nu)$. We express $(\mu - \nu)$ as τ:

$$\tau = \mu - \nu. \tag{11}$$

τ is difference between the unit-cell number μ and ν. $a_1(\tau)$ is calculated by numerical integration of concrete expression of Eq. 10, that is,

$$a_1(\tau) = \frac{1}{2\pi}\int_{-\pi}^{\pi} \frac{\cos(\tau k)}{\sqrt{3 + 2\cos k}}\mathrm{d}k. \tag{12}$$

$a_2(\tau)$ is zero, because $C_2(k)$ is zero. $a_3(\tau)$ is calculated by using following relation:

$$a_3(\tau) = -a_1(\tau) - \frac{1}{2}\{a_1(\tau + 1) + a_1(\tau - 1)\}. \tag{13}$$

This relation was confirmed by using the addition theorem of exponential function. We note that $a_r(\tau)$ are even functions with respect to τ, that is,

$$a_r(\tau) = a_r(-\tau). \tag{14}$$

This is supported by Eqs. 8 and 10.

τ dependence of $a_r(\tau)$ in **1** is shown in Fig. 3. We can see that each $a_r(\tau)$ $(r = 1, 3)$ decreased when the absolute value of τ increased. In particular, $a_r(\tau)$ with $|\tau| \geq 2$ were trivial compared with $a_r(0)$ and $a_r(1)$. This means that the ν-th Wannier function is localized only at $(\nu \pm 1)$-th cells, that is,

$$0 < \ldots |a_r(-3)| < |a_r(-2)| \ll |a_r(-1)| < |a_r(0)| > |a_r(1)| \gg |a_r(2)| > |a_r(3)| \ldots > 0. \tag{15}$$

Therefore, we supposed that:

$$a_r(\tau) = 0 \quad \text{when} \quad |\tau| \geq 2. \tag{16}$$

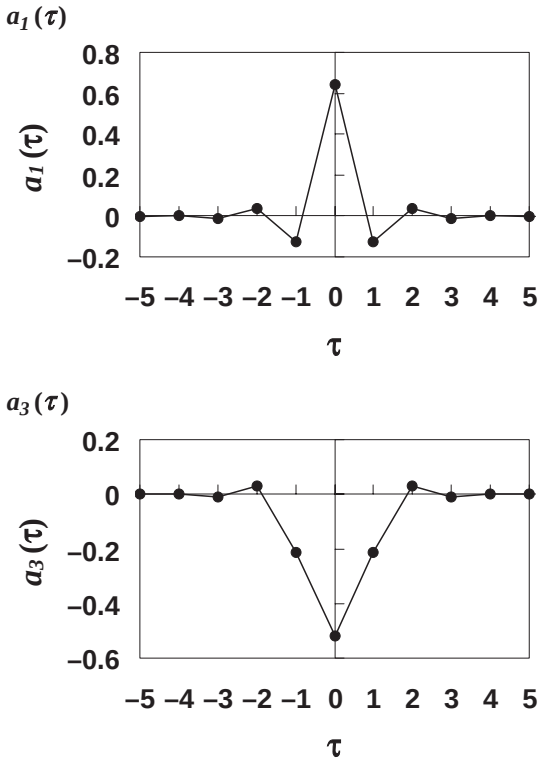

Fig. 3. Wannier-function coefficients of **1**. Both $a_1(\tau)$ and $a_3(\tau)$ rapidly decayed when $|\tau| \geq 2$.

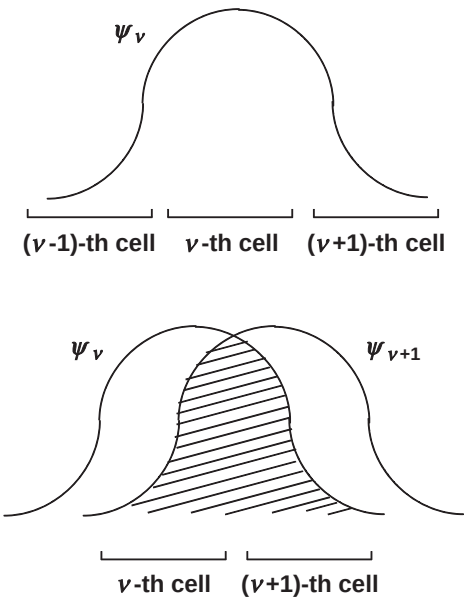

Fig. 4. Degree of localization in the Wannier functions. The ν-th Wannier function ψ_ν is spread over $(\nu \pm 1)$-th cells. In nondisjoint polymers, the ν-th and $(\nu + 1)$-th Wannier-functions (ψ_ν and $\psi_{\nu+1}$) overlap each other between ν-th and $(\nu + 1)$-th cells.

This situation is schematically illustrated in Fig. 4. The ν-th Wannier function ψ_ν was localized at the $(\nu \pm 1)$-th cells. Similarly, the $(\nu + 1)$-th Wannier function $\psi_{\nu+1}$ was localized at the $\{(\nu + 1) \pm 1\}$-th cells. Then, ψ_ν and $\psi_{\nu+1}$ overlap each other between the ν-th and $(\nu + 1)$-th cells expressed by

Fig. 5. Electronic configuration of ferromagnetic states in nondisjoint polymers.

shadow. As is shown later, the overlap between ν-th and $(\nu+1)$-th Wannier functions is formulated as two-electron wave function $PNBCO_{\nu,\nu+1}$, and plays an important role in ferromagnetic interactions in non-Kekulé polymers.

The electronic configuration of the ferromagnetic state of the polymer **1** by using the Wannier functions is described in Fig. 5. We note that simultaneous occupancy of two electrons with parallel spin at the same Wannier function is forbidden by the Pauli principle. Therefore, ferromagnetic interactions occur between two Wannier functions with different index ν. The overlaps between the Wannier functions, that is, product of Wannier functions, did not vanish only between the ν-th and $(\nu+1)$-th cells, as mentioned above. Therefore, we focused on amplitude pattern in the product of the Wannier functions $\psi_\nu\psi_{\nu+1}$, as described below.

We constructed two-electron wave function by product of the ν-th and $(\nu+1)$-th Wannier functions as $PNBCO_{\nu,\nu+1}$:

$$\begin{aligned}
&PNBCO_{\nu,\nu+1}\\
&= \psi_\nu(\mathbf{1})\psi_{\nu+1}(\mathbf{2})\\
&= \left(\sum_{\mu}^{N}\sum_{r}^{n} a_r(\mu-\nu)\chi_{\mu,r}(\mathbf{1})\right)\\
&\quad\times\left(\sum_{\mu'}^{N}\sum_{s}^{n} a_s(\mu'-\nu-1)\chi_{\mu',s}(\mathbf{2})\right)\\
&= \left(\sum_{\tau+\nu}^{N}\sum_{r}^{n} a_r(\tau)\chi_{\tau+1,r}(\mathbf{1})\right)\left(\sum_{\tau'+\nu'}^{N}\sum_{s}^{n} a_s(\tau'-1)\chi_{\tau'+\nu,s}(\mathbf{2})\right)\\
&\cong \left(\sum_{\tau}^{-1,0,1}\sum_{r}^{n} a_r(\tau)\chi_{\tau+\nu,r}(\mathbf{1})\right)\left(\sum_{\tau'}^{0,1,2}\sum_{s}^{n} a_s(\tau'-1)\chi_{\tau'+\nu,s}(\mathbf{2})\right)\\
&= \left[\sum_{r}^{n}\{a_r(-1)\chi_{\nu-1,r}(\mathbf{1})+a_r(0)\chi_{\nu,r}(\mathbf{1})+a_r(1)\chi_{\nu+1,r}(\mathbf{1})\}\right]\\
&\quad\times\left[\sum_{s}^{n}\{a_s(-1)\chi_{\nu,s}(\mathbf{2})+a_s(0)\chi_{\nu+1,s}(\mathbf{2})+a_s(1)\chi_{\nu+2,s}(\mathbf{2})\}\right],
\end{aligned}\tag{17}$$

where Equation 16 was applied in the approximation. The electron number "**1**" and "**2**" were added as bold letters for clarification. Equation 17 is further approximated using the "neglect of differential overlap" (NDO) as follows:

$$\begin{aligned}
PNBCO_{\nu,\nu+1} &\cong C\left[\sum_{r}^{\nu\text{-th cell}}\{a_r(-1)a_r(0)\chi_{\nu,r}(\mathbf{1})\chi_{\nu,r}(\mathbf{2})\}\right.\\
&\qquad\left.+\sum_{r}^{(\nu+1)\text{-th cell}}\{a_r(0)a_r(1)\chi_{\nu+1,r}(\mathbf{1})\chi_{\nu+1,r}(\mathbf{2})\}\right]\\
&= C\left[\sum_{r}^{\nu\text{-th cell}}\{a_r(0)a_r(1)\chi_{\nu,r}(\mathbf{1})\chi_{\nu,r}(\mathbf{2})\}\right.\\
&\qquad\left.+\sum_{r}^{(\nu+1)\text{-th cell}}\{a_r(0)a_r(1)\chi_{\nu+1,r}(\mathbf{1})\chi_{\nu+1,r}(\mathbf{2})\}\right].
\end{aligned}\tag{18}$$

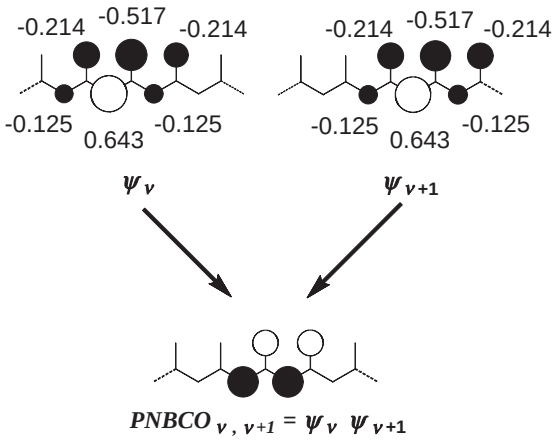

Fig. 6. Schematic representation of the ν-th and $(\nu+1)$-th Wannier-functions (ψ_ν and $\psi_{\nu+1}$) in **1**. Their product $PNBCO_{\nu,\nu+1}$ is also shown.

In the last expression, even-function character of $a_r(\tau)$ (Eq. 14) was applied. We note that the first and second summations in the last expression are taken in the ν-th and $(\nu+1)$-th cell, respectively. C is chosen so that $PNBCO_{\nu,\nu+1}$ is normalized under the NDO approximation. NDO approximation is useful for description of non-Kekulé systems.[11] The last expression in Eq. 18 makes it possible to obtain schematic representation of $PNBCO_{\nu,\nu+1}$ by simple product between the coefficients on the same atomic site in the ν-th and $(\nu+1)$-th cells.

Figure 6 shows the amplitude pattern of ψ_ν, $\psi_{\nu+1}$, and $PNBCO_{\nu,\nu+1}$ of **1**. Since the NDO approximation was applied, the $PNBCO_{\nu,\nu+1}$ contained only ionic terms, that is, $\chi_{\nu,r}(\mathbf{1})\chi_{\nu,r}(\mathbf{2})$ and $\chi_{\nu+1,r}(\mathbf{1})\chi_{\nu+1,r}(\mathbf{2})$. Therefore, the squared amplitudes of the $PNBCO_{\nu,\nu+1}$ represent the instabilities of the anti-parallel-spin states. In short, since simultaneous occupancy of two electrons with parallel spin at the same atomic orbital is forbidden by the Pauli principle, resultant reduction of Coulomb repulsion leads to parallel-spin preference in $PNBCO_{\nu,\nu+1}$. This situation resembles that in nondisjoint biradicals, in which the squared amplitudes of the product of NBMOs (PNBMO) represent singlet instabilities.[6,11] Nondisjoint-type biradicals have triplet ground states, and the sum of the squared amplitudes of PNBMO is approximately proportional to the exchange integral between two NBMOs.[6,11] Therefore, apart from the normalization factor, the sum of the squared amplitudes of $PNBCO_{\nu,\nu+1}$ is considered to be approximately proportional to exchange integral between the two Wannier functions ψ_ν and $\psi_{\nu+1}$. Such a consideration is in line with recent studies of high-spin oligomers and/or polymers using the L_{ij} index.[6,20,21] Although the L_{ij} index has been defined in oligomers and extended to polymers by extrapolation,[6,20,21] $PNBCO_{\nu,\nu+1}$ is formulated in infinite systems under the periodic boundary condition. In **1**, ψ_ν and $\psi_{\nu+1}$ are nondisjoint, because the product between them, that is, $PNBCO_{\nu,\nu+1}$ is not zero.

We next explain through-space interactions in non-Kekulé polymers analyzing **1**. The through-space interactions are deduced by focusing on amplitude pattern of the $PNBCO_{\nu,\nu+1}$. The antibonding through-space interactions in $PNBCO_{\nu,\nu+1}$ stabilized the ferromagnetic state. The $PNBCO_{\nu,\nu+1}$ of **1** contained in-phase and out-of-phase moieties created by the non-nearest-neighbor atomic sites as depicted in Fig. 7. The in-phase and out-of-phase moieties are described as "P_{sym}-fragment" and "P_{anti}-fragment," respectively, in Fig. 7. P_{sym}-fragments and P_{anti}-fragments influence anti-parallel-spin state in each $PNBCO_{\nu,\nu+1}$ via through-space interactions. In short, the anti-parallel-spin states are stabilized by P_{sym}-fragments and destabilized by P_{anti}-fragments, analogous to through-space interactions in nondisjoint biradicals.[11] Of all non-nearest-neighbor atomic sites, only the second-nearest-neighbor atomic sites significantly contribute to through-space interactions.[11]

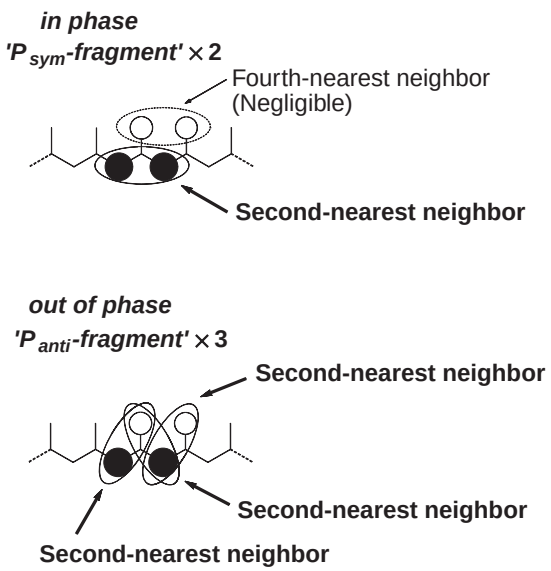

Fig. 7. Through-space interactions in $PNBCO_{\nu,\nu+1}$ of **1**. Whereas in-phase moiety "P_{sym}-fragment" contribute to anti-parallel-spin preference, the out-of-phase moiety "P_{anti}-fragment" contribute to parallel-spin preference.

Therefore, the interactions between the fourth-nearest-neighbor atomic sites are negligible, as indicated in Fig. 7. It can be seen from Fig. 1 and Fig. 7 that the P_{anti}-fragments always appear around the "unstarred atoms." In nondisjoint systems, the P_{anti}-fragments are created by orbital mixing.[11] This can be schematically explained analyzing nondisjoint biradical **2**. That is, linkage of "starred atoms" to "unstarred atoms" leads to orbital mixing, which creates in-phase and out-of-phase moieties in the NBMOs,[11] as seen from Fig. 2. Then, resultant product of NBMOs (PNBMO) contain an out-of-phase fragment, that is, P_{anti}-fragment. In general, at least one P_{anti}-fragment appears around the "unstarred atoms" in PNBMO of nondisjoint biradicals.[11] Then, PNBMO in nondisjoint biradicals becomes rich in antibonding character. This situation has been clarified by using unitary transformation of NBMOs.[11] Similarly, in extended systems, $PNBCO_{\nu,\nu+1}$ becomes antibonding rich, as shown in Fig. 7. Moreover, in nondisjoint systems, the destabilization energy due to P_{anti}-fragments is larger than the stabilization energy due to P_{sym}-fragments.[11] Therefore, in non-Kekulé polymers, through-space interactions in P_{anti}-fragments are more significant than those in P_{sym}-fragments.

Next, as another example of nondisjoint polymer, the Wannier functions and $PNBCO_{\nu,\nu+1}$ of **3** are shown in Fig. 8. The derivation of the Wannier functions is given in appendix. The amplitude-pattern analysis is similarly described in Fig. 9. From Fig. 9, we can see that the number of P_{anti}-fragments is larger than that of P_{sym}-fragments. That is, the $PNBCO_{\nu,\nu+1}$ is also rich in antibonding character.

In contrast to nondisjoint polymer **1** and **3**, $PNBCO_{\nu,\nu+1}$ of disjoint polymers vanished under the NDO approximation. This was shown by analyzing disjoint polymer **5**. The nonbonding Bloch functions of **5** were independent of wavenumber k, and each Wannier function was localized only on one unit cell. The derivation of this situation was given in appendix. Each $PNBCO_{\nu,\nu+1}$ vanished, because $PNBCO_{\nu,\nu+1}$ created between adjacent cells does not overlap each other. This situation is schematically described in Fig. 10. In such a case, anti-parallel-spin states in $PNBCO_{\nu,\nu+1}$ are not destabilized. Indeed, derivatives of **5** did not show ferromagnetic spin align-

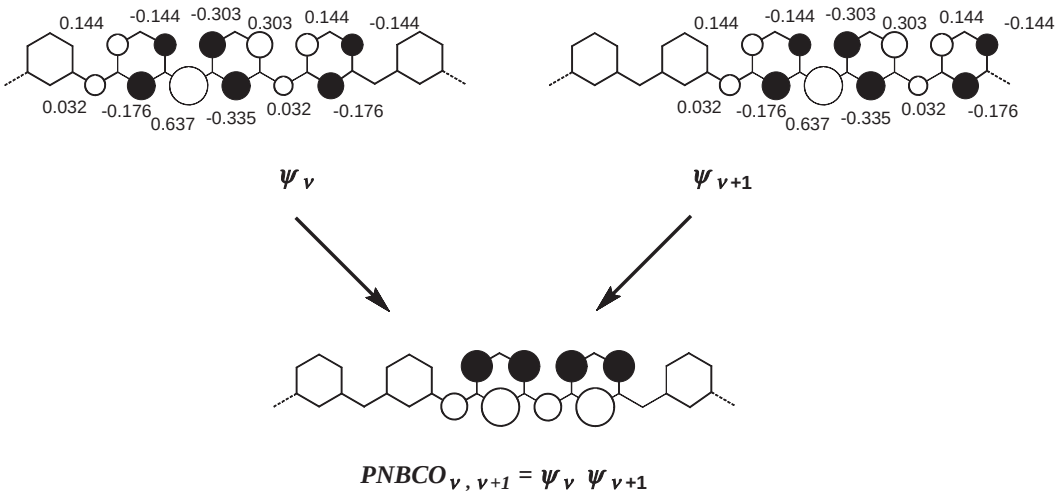

Fig. 8. Schematic representation of the ν-th and $(\nu + 1)$-th Wannier-functions (ψ_ν and $\psi_{\nu+1}$) in **3**. Their product $PNBCO_{\nu,\nu+1}$ was also shown.

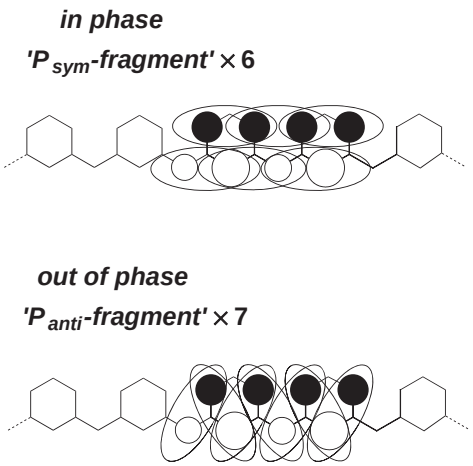

Fig. 9. Through-space interactions in $PNBCO_{\nu,\nu+1}$ of **3**. Whereas in-phase moiety "P_{sym}-fragment" contribute to anti-parallel-spin preference, the out-of-phase moiety "P_{anti}-fragment" contribute to parallel-spin preference.

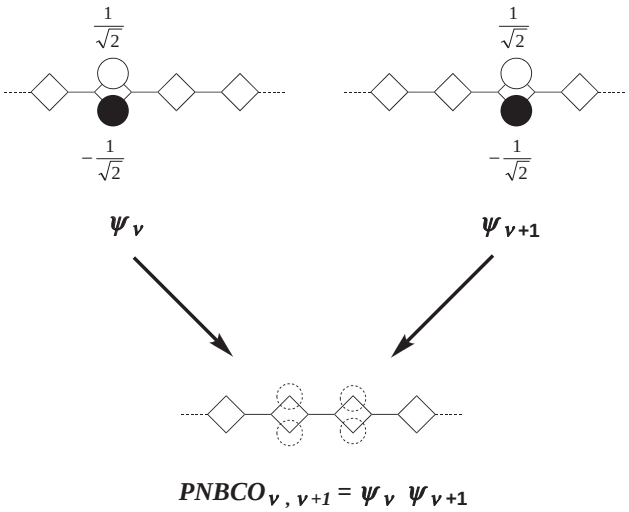

Fig. 10. Schematic representation of the ν-th and $(\nu+1)$-th Wannier-functions (ψ_ν and $\psi_{\nu+1}$) in **5**. Their product $PNBCO_{\nu,\nu+1}$ vanishes, because ψ_ν and $\psi_{\nu+1}$ are localized only at one unit cell.

ment.[17] Through-space interactions in $PNBCO_{\nu,\nu+1}$ are also trivial in disjoint polymers.

In the next section, through-space interactions described above are clarified by introducing overlap integral into $PNBCO_{\nu,\nu+1}$.

Discussion

Since $PNBCO_{\nu,\nu+1}$ vanishes in disjoint polymers, hereafter, we focused on nondisjoint polymers. Through-space interactions in $PNBCO_{\nu,\nu+1}$ are formulated by taking into account overlap integral, because the interactions occur between non-nearest-neighbor carbon atomic sites. Taking into account the overlap integral s_{st} between atomic site s and t, $PNBCO_{\nu,\nu+1}$ in Eq. 18 is extended as follows:

$$PNBCO_{\nu,\nu+1} \cong \frac{C\left[\sum_{r}^{\nu\text{-th cell}} \{a_r(0)a_r(1)\chi_{\nu,r}(\mathbf{1})\chi_{\nu,r}(\mathbf{2})\} + \sum_{r}^{(\nu+1)\text{-th cell}} \{a_r(0)a_r(1)\chi_{\nu+1,r}(\mathbf{1})\chi_{\nu+1,r}(\mathbf{2})\}\right]}{\sqrt{1+Z_{\nu,\nu+1}}}, \quad (19)$$

where $Z_{\nu,\nu+1}$ is:

$$Z_{\nu,\nu+1} = 2C^2\left[\begin{array}{l} \sum_{s\neq t}^{\nu\text{-th cell}} \{a_s(0)a_s(1)\}\{a_t(0)a_t(1)\}+ \\ \sum_{s\neq t}^{(\nu+1)\text{-th cell}} \{a_s(0)a_s(1)\}\{a_t(0)a_t(1)\}+ \\ \sum_{s\neq t}^{\nu\text{-th and }(\nu+1)\text{-th cell}} \{a_s(0)a_s(1)\}\{a_t(0)a_t(1)\} \end{array}\right] {s_{st}}^2 \quad (20)$$

In Eq. 20, the first and second summations are taken in the ν-th and $(\nu+1)$-th cell, respectively, and the third summation is taken between the ν-th and $(\nu+1)$-th cells.

Then, square of $PNBCO_{\nu,\nu+1}$ becomes:

$$\begin{aligned} {PNBCO_{\nu,\nu+1}}^2 &\cong (1+Z_{\nu,\nu+1})^{-1} \\ &\times C\left[\sum_{r}^{\nu\text{-th cell}} \{a_r(0)a_r(1)\chi_{\nu,r}(\mathbf{1})\chi_{\nu,r}(\mathbf{2})\} + \sum_{r}^{(\nu+1)\text{-th cell}} \{a_r(0)a_r(1)\chi_{\nu+1,r}(\mathbf{1})\chi_{\nu+1,r}(\mathbf{2})\}\right] \\ &\times C\left[\sum_{s}^{\nu\text{-th cell}} \{a_s(0)a_s(1)\chi_{\nu,s}(\mathbf{1})\chi_{\nu,s}(\mathbf{2})\} + \sum_{s}^{(\nu+1)\text{-th cell}} \{a_s(0)a_s(1)\chi_{\nu+1,s}(\mathbf{1})\chi_{\nu+1,s}(\mathbf{2})\}\right] \\ &\cong C^2(1-Z_{\nu,\nu+1}) \\ &\times \left[\sum_{r}^{\nu\text{-th cell}} \{a_r(0)^2a_r(1)^2\chi_{\nu,r}(\mathbf{1})^2\chi_{\nu,r}(\mathbf{2})^2\} + \sum_{r}^{(\nu+1)\text{-th cell}} \{a_r(0)^2a_r(1)^2\chi_{\nu+1,r}(\mathbf{1})^2\chi_{\nu+1,r}(\mathbf{2})^2\}\right], \end{aligned} \quad (21)$$

under the NDO approximation. The term $(1-Z_{\nu,\nu+1})$ resulted from Taylor expansion with respect to $Z_{\nu,\nu+1}$.

The squared amplitudes of $PNBCO_{\nu,\nu+1}$ in Eq. 21 also represent instabilities of the anti-parallel-spin state, because Equation 21 includes only square of ionic terms, that is, $\chi_{\nu,r}(\mathbf{1})^2\chi_{\nu,r}(\mathbf{2})^2$ and $\chi_{\nu+1,r}(\mathbf{1})^2\chi_{\nu+1,r}(\mathbf{2})^2$. We can see from Eq. 21 that the squared amplitude of $PNBCO_{\nu,\nu+1}$ is influenced by $Z_{\nu,\nu+1}$. $Z_{\nu,\nu+1}$ depends on amplitude pattern of $PNBCO_{\nu,\nu+1}$ as described below.

In Eq. 20, the term $a_s(0)a_s(1)a_t(0)a_t(1)$ is product of the s-th

and t-th $PNBCO_{\nu,\nu+1}$ amplitudes. This term is positive when the s-th and t-th $PNBCO_{\nu,\nu+1}$ amplitudes have the same sign. Oppositely, the term is negative when the s-th and t-th $PNBCO_{\nu,\nu+1}$ amplitudes have different sign. Therefore, the term $a_s(0)a_s(1)a_t(0)a_t(1)$ is positive in P_{sym}-fragments and negative in P_{anti}-fragments, respectively. Thus, from Eq. 21, P_{sym}-fragments decrease the anti-parallel-spin instabilities. In other words, bonding interactions in P_{sym}-fragments stabilize anti-parallel-spin states. Oppositely, P_{anti}-fragments increase the anti-parallel-spin instabilities, i.e., antibonding interactions in P_{anti}-fragments destabilize anti-parallel-spin states. This means that P_{anti}-fragments contribute to parallel-spin preference. Thus, through-space interactions in $PNBCO_{\nu,\nu+1}$ influence the anti-parallel-spin states. In particular, through-space interactions in P_{anti}-fragments are ferromagnetic.

Again, from Figs. 7 and 9, we can see that the number of P_{anti}-fragments is larger than that of P_{sym}-fragments. This is characteristic of nondisjoint systems, as mentioned above. Then, through-space interactions in $PNBCO_{\nu,\nu+1}$ become antibonding rich. Therefore, $Z_{\nu,\nu+1}$ is negative and:

$$(1 - Z_{\nu,\nu+1}) > 1. \tag{22}$$

Thus, from Eq. 21, the degree of anti-parallel-spin instabilities, that is, the squared amplitude of $PNBCO_{\nu,\nu+1}$, increases by antibonding-through-space interactions. The instabilities are based on Coulomb repulsions in anti-parallel-spin states in $PNBCO_{\nu,\nu+1}$, as mentioned above. Then, the instabilities in anti-parallel-spin states of $PNBCO_{\nu,\nu+1}$ consist of "on-site term" and "through-space term." The former corresponds to squared amplitude of the same atomic site on $PNBCO_{\nu,\nu+1}$, and the latter corresponds to antibonding-through-space interactions due to $Z_{\nu,\nu+1}$ in $PNBCO_{\nu,\nu+1}$. This situation is expressed as follows:

$$|PNBCO_{\nu,\nu+1}|^2 \cong |PNBCO_{\nu,\nu+1}|^2(\text{on-site term}) + |PNBCO_{\nu,\nu+1}|^2(\text{through-space term}). \tag{23}$$

Strictly speaking, vibronic interactions characteristic of degenerate systems[23] may play some roles in the instabilities. However, their contributions to the ferromagnetic interactions are probably small, because the non-bonding characters in many non-Kekulé systems are essentially conserved even if they are subject to Jahn–Teller and/or Peierls distortions.[8,17,24]

Thus, ferromagnetic interactions in periodic-non-Kekulé polymers were attributed to the relaxation of Coulomb repulsions in anti-parallel-spin states in $PNBCO_{\nu,\nu+1}$.

Conclusion

Ferromagnetic interactions in non-Kekulé polymers were analyzed under the periodic boundary condition. The product of the ν-th and $(\nu+1)$-th Wannier functions was defined as $PNBCO_{\nu,\nu+1}$ (product of NBCOs). We showed that squared amplitudes of $PNBCO_{\nu,\nu+1}$ represented the instabilities of anti-parallel-spin states. The instabilities were due to Coulomb repulsions in anti-parallel-spin states. In nondisjoint polymers, the instabilities consisted of an "on-site term," which corresponded to the squared amplitude on the same atomic site in $PNBCO_{\nu,\nu+1}$, and a "through-space term," which corresponded to the antibonding-through-space interactions in $PNBCO_{\nu,\nu+1}$. Such instabilities led to ferromagnetic interactions. On the other hand, in disjoint polymers, such instabilities did not emerge.

Appendix

Bloch functions and Wannier functions of **3** are deduced by solving secular equation as follows:

$$\begin{vmatrix} x & 1 & 0 & 0 & 0 & e^{ik} & 0 \\ 1 & x & 1 & 0 & 0 & 0 & 1 \\ 0 & 1 & x & 1 & 0 & 0 & 0 \\ 0 & 0 & 1 & x & 1 & 0 & 0 \\ 0 & 0 & 0 & 1 & x & 1 & 0 \\ e^{-ik} & 0 & 0 & 0 & 1 & x & 1 \\ 0 & 1 & 0 & 0 & 0 & 1 & x \end{vmatrix} = 0. \tag{A-1}$$

From Eq. A1, we obtained the non-bonding Bloch functions corresponding to $x = 0$:

$$C_1(k) = \frac{2}{\sqrt{10 - 2\cos k}}, \tag{A-2}$$

$$C_3(k) = -C_5(k) = -\frac{1 - e^{-ik}}{\sqrt{10 - 2\cos k}}, \tag{A-3}$$

$$C_7(k) = -\frac{1 + e^{-ik}}{\sqrt{10 - 2\cos k}}, \tag{A-4}$$

$$C_2(k) = C_4(k) = C_6(k) = 0 \tag{A-5}$$

Although the complex conjugates of these Bloch functions are consistent with those in the literature,[16] they are still complex numbers. We needed to adopt their real parts so that corresponding Wannier functions became even functions with respect to τ. The real parts of them were made by Eq. 8, and corresponding Wannier functions satisfied following relations.

$$a_1(\tau) = \frac{1}{2\pi}\int_{-\pi}^{\pi} \frac{2\cos(\tau k)}{\sqrt{10 - 2\cos k}}\,\mathrm{d}k, \tag{A-6}$$

$$a_3(\tau) = -a_5(\tau) = -\frac{1}{2}a_1(\tau) + \frac{1}{4}\{a_1(\tau+1) + a_1(\tau-1)\}, \tag{A-7}$$

$$a_7(\tau) = -\frac{1}{2}a_1(\tau) - \frac{1}{4}\{a_1(\tau+1) + a_1(\tau-1)\}, \tag{A-8}$$

$$a_2(\tau) = a_4(\tau) = a_6(\tau) = 0. \tag{A-9}$$

Similarly, non-bonding Bloch and Wannier functions of **5** were determined by solving secular equation as follows:

$$\begin{vmatrix} x & 1 & e^{ik} & 1 \\ 1 & x & 1 & 0 \\ e^{-ik} & 1 & x & 1 \\ 1 & 0 & 1 & x \end{vmatrix} = 0. \tag{A-10}$$

When $x = 0$, we obtained:

$$C_1(k) = C_3(k) = 0, \tag{A-11}$$

$$C_2(k) = -C_4(k) = \frac{1}{\sqrt{2}}, \tag{A-12}$$

$$a_1(\tau) = a_3(\tau) = 0, \tag{A-13}$$

$$a_2(\tau) = -a_4(\tau) = \frac{1}{2\pi}\int_{-\pi}^{\pi} \exp\{i(\mu - \nu)\}\left(\frac{1}{\sqrt{2}}\right)\mathrm{d}k = \frac{1}{\sqrt{2}}\delta_{\mu\nu} \quad (\tau = \mu - \nu). \tag{A-14}$$

Each Wannier function is localized only at one unit cell due to the Kronecker's delta.

References

1 N. Mataga, *Theor. Chim. Acta* **1968**, *10*, 372.
2 A. A. Ovchinnikov, *Theor. Chim. Acta* **1978**, *47*, 297.
3 N. Tyutyulkov, P. Schuster, O. Polansky, *Theor. Chim. Acta* **1983**, *63*, 291.
4 W. T. Borden, E. R. Davidson, *J. Am. Chem. Soc.* **1977**, *99*, 4587.
5 W. T. Borden, *Mol. Cryst. Liq. Cryst.* **1993**, *232*, 195.
6 Y. Aoki, A. Imamura, *Int. J. Quantum Chem.* **1999**, *74*, 491.
7 P. Dowd, *Acc. Chem. Res.* **1972**, *5*, 242.
8 M. Hatanaka, R. Shiba, *J. Comput. Chem., Jpn.* **2006**, *5*, 171.
9 H. Iwamura, *Adv. Phys. Org. Chem.* **1990**, *26*, 179.
10 A. Rajca, *Chem. Rev.* **1994**, *94*, 871.
11 M. Hatanaka, R. Shiba, *Bull. Chem. Soc. Jpn.* **2007**, *80*, 1750.
12 H. Murata, D. Miyajima, R. Takada, H. Nishide, *Polym. J.* **2005**, *37*, 818.
13 M. Hatanaka, R. Shiba, *J. Comput. Chem., Jpn.* **2005**, *4*, 101.
14 J. Pranata, *J. Am. Chem. Soc.* **1992**, *114*, 10537.
15 K. Yoshizawa, T. Kuga, T. Sato, M. Hatanaka, K. Tanaka, T. Yamabe, *Bull. Chem. Soc. Jpn.* **1996**, *69*, 3443.
16 N. N. Tyutyulkov, S. C. Karabunarliev, *Int. J. Quantum Chem.* **1986**, *29*, 1325.
17 J. Pranata, D. A. Dougherty, *J. Am. Chem. Soc.* **1987**, *109*, 1621.
18 A. Rajca, J. Wongsriratanakul, S. Rajca, *Science* **2001**, *294*, 1503.
19 S. Rajca, A. Rajca, *J. Solid State Chem.* **2001**, *159*, 460.
20 Y. Orimoto, T. Imai, K. Naka, Y. Aoki, *J. Phys. Chem. A* **2006**, *110*, 5803.
21 Y. Orimoto, Y. Aoki, *J. Chem. Theory Comput.* **2006**, *2*, 786.
22 F. Dietz, N. Tyutyulkov, *Chem. Phys.* **2001**, *264*, 37.
23 T. Kato, T. Yamabe, *J. Chem. Phys.* **2001**, *115*, 8592.
24 K. Yoshizawa, M. Hatanaka, Y. Matsuzaki, K. Tanaka, T. Yamabe, *J. Chem. Phys.* **1994**, *100*, 4453.